Journal of Environmental Management 144 (2014) 226–235

Contents lists available at ScienceDirect

Journal of Environmental Management

journal homepage: www.elsevier.com/locate/jenvman

Modeling vegetation heights from high resolution stereo aerial photography: An application for broad-scale rangeland monitoring

Jeffrey K. Gillan [a, *], Jason W. Karl [a], Michael Duniway [b], Ahmed Elaksher [c]

[a] United States Department of Agriculture – Agricultural Research Service (USDS-ARS), Jornada Experimental Range, P.O. Box 30003, MSC 3JER, New Mexico State University, Las Cruces, NM 88003-8003, USA
[b] U.S. Geological Survey, Southwest Biological Science Center, 2290 SW Resource Blvd. Moab, UT 84532, USA
[c] New Mexico State University, Department of Engineering Technology and Surveying Engineering, P.O. Box 30001, MSC 3566, Las Cruces, NM 88003-8001, USA

ARTICLE INFO

Article history:
Received 13 September 2013
Received in revised form
16 May 2014
Accepted 25 May 2014
Available online

Keywords:
Rangeland monitoring
Photogrammetry
Vegetation height
Digital terrain model
Remote sensing

ABSTRACT

Vertical vegetation structure in rangeland ecosystems can be a valuable indicator for assessing rangeland health and monitoring riparian areas, post-fire recovery, available forage for livestock, and wildlife habitat. Federal land management agencies are directed to monitor and manage rangelands at landscapes scales, but traditional field methods for measuring vegetation heights are often too costly and time consuming to apply at these broad scales. Most emerging remote sensing techniques capable of measuring surface and vegetation height (e.g., LiDAR or synthetic aperture radar) are often too expensive, and require specialized sensors. An alternative remote sensing approach that is potentially more practical for managers is to measure vegetation heights from digital stereo aerial photographs. As aerial photography is already commonly used for rangeland monitoring, acquiring it in stereo enables three-dimensional modeling and estimation of vegetation height. The purpose of this study was to test the feasibility and accuracy of estimating shrub heights from high-resolution (HR, 3-cm ground sampling distance) digital stereo-pair aerial images. Overlapping HR imagery was taken in March 2009 near Lake Mead, Nevada and 5-cm resolution digital surface models (DSMs) were created by photogrammetric methods (aerial triangulation, digital image matching) for twenty-six test plots. We compared the heights of individual shrubs and plot averages derived from the DSMs to field measurements. We found strong positive correlations between field and image measurements for several metrics. Individual shrub heights tended to be underestimated in the imagery, however, accuracy was higher for dense, compact shrubs compared with shrubs with thin branches. Plot averages of shrub height from DSMs were also strongly correlated to field measurements but consistently underestimated. Grasses and forbs were generally too small to be detected with the resolution of the DSMs. Estimates of vertical structure will be more accurate in plots having low herbaceous cover and high amounts of dense shrubs. Through the use of statistically derived correction factors or choosing field methods that better correlate with the imagery, vegetation heights from HR DSMs could be a valuable technique for broad-scale rangeland monitoring needs.

1. Introduction

Quantitatively measured ecosystem indicators of soil, vegetation, and ground cover characteristics are essential for tracking the basic ecological functions and associated ecosystem services provided by rangelands (National Research Council, 1994; Herrick et al., 2010). Vegetation heights are an important indicator of habitat quality for many wildlife species. For example, Greater Sage-grouse (*Centrocercus urophasianus*) require specific sagebrush (*Artemisia* spp.) heights for successful nesting and brood-rearing (Connelly et al., 2000). Burrowing owls (*Athene cunicularia*) use vegetation around nest sites as elevated perches to detect both prey and predators (Green and Anthony, 1989). Vegetation height can be used to estimate above-ground biomass (Cleary et al., 2008) which is in turn used to determine total available forage (Karl and Nicholson, 1987), browse (Bryant and Kothmann, 1979), available

* Corresponding author. Tel.: +1 575 646 2961, fax: +1 575 646 5889.
E-mail address: jgillan@nmsu.edu (J.K. Gillan).

http://dx.doi.org/10.1016/j.jenvman.2014.05.028
0301-4797/

fuel for controlled or uncontrolled burning (Riaño et al., 2007; Leis and Morrison, 2011), and carbon storage (Asner et al., 2003; Brown et al., 2005). Height of vegetation is also an important variable in determining wind erosion potential for arid and semi-arid lands (Okin, 2008).

Nationwide efforts to monitor vegetation heights on public and privately owned rangelands such as the National Resources Inventory (NRI, Nusser and Goebel, 1997) and Bureau of Land Management Assessment, Inventory and Monitoring (BLM AIM, Toevs et al., 2011) programs in the United States rely on field measurements from thousands of sample locations. Due to costs associated with field visits and the improving availability and resolution of remotely sensed imagery, measurement tools from aerial and satellite-based image products are being sought (Hunt et al., 2003; Booth and Cox, 2008) to expand monitoring coverage.

A variety of quantitative indicators derived from either image interpretation, classification, or modeling have been shown to be accurate, feasible, cost-effective, and repeatable compared to field methods especially when applied to high-resolution (e.g., ground-sampling distance [GSD] of less than 1 m but greater than 1 cm) and very-high-resolution (i.e., GSD less than 1 cm) imagery (House et al., 1998; Seefeldt and Booth, 2006; Luscier et al., 2006; Booth and Cox, 2008; Duniway et al., 2011; Karl et al., 2012a, 2012b). Some of these indicators include vegetation cover, composition, and canopy gap sizes.

Accurate estimation of vegetation height via remote sensing in arid and semi-arid ecosystems, however, has been limited. Some studies have used "small footprint" LiDAR (i.e., airborne scanning laser with point densities ranging from 0.54 to 9.46 points per m^2) to estimate shrub canopy characteristics (Streutker and Glenn, 2006; Riaño et al., 2007; Su and Bork, 2007; Glenn et al., 2011; Mitchell et al., 2011; Sankey and Bond, 2011). These studies all found strong relationships between field-measured and LiDAR-estimated shrub heights, but reported that LiDAR methods consistently underestimated shrub height (and in the case of Mitchell et al. shrub area). Others studies have correlated field-based sagebrush and bitterbrush heights with spectra from satellite-based image products (2.4 m Quickbird, 20 m SPOT, 30 m Landsat TM, 56 m AWiFS), with limited success (Jakubauskas et al., 2001; Homer et al., 2012). Results varied by spectral band, targeted species, and vegetation phenology.

Vegetation height can also be estimated via aerial photogrammetry. Though traditionally used to determine and map topographic relief from sets of overlapping (i.e., stereo) aerial photographs (Wolf and Dewitt, 2000), photogrammetric approaches to estimating vegetation height has been demonstrated in forests (Gong et al., 2000; Miller et al., 2000; Brown et al., 2005; Massada et al., 2006) and mangroves (Lucas et al., 2002; Mitchell et al., 2007). Application of aerial photogrammetric approaches has not been widely applied to estimating heights or canopy characteristics of shrubs in arid and semi-arid environments because it requires very high resolution (e.g., GSD < 5 cm) images. However, the availability of higher-resolution digital mapping cameras as well as increasing use of unmanned aerial vehicles (Rango et al., 2009) or piloted light aircraft (Booth et al., 2003) for collecting very large scale aerial imagery has opened up new possibilities for estimating heights of individual shrubs from stereo aerial photography.

The relative strengths and limitations of measuring vegetation heights through aerial photogrammetry must be better understood to be compared against alternate technologies such as LiDAR. A major advantage of aerial photogrammetry is its ability to capture heights as well as spectral information simultaneously. Established monitoring programs like the NRI that are already acquiring aerial imagery for other purposes (Nusser and Goebel, 1997) could be tasked to capture the imagery in stereo. A potential drawback, however, is that photogrammetric techniques cannot model different canopy layers whereas LiDAR can (Reutebuch et al., 2005). Photogrammetric methods can only depict the tops of vegetation and provide little information on the understory. How this would affect vegetation height estimation and its utility in arid and semi-arid environmental monitoring is not known. Compared with published LiDAR studies, available stereo aerial photography has higher spatial resolution for distinguishing vegetation height, but its accuracy and resolving power need to be explored further.

Our objective for this study was to determine the ability to accurately estimate vegetation heights using high-resolution stereo aerial photography at individual-shrub and plot scales. We compare vegetation height models created from digital stereo aerial photography with field measurements in the Mojave Desert (Nevada and California, USA) and discuss limitations and applications of the technique for broad-scale ecosystem monitoring.

2. Materials and methods

2.1. Study area

This study was conducted in the Lake Mead National Recreation Area (LMNRA), Nevada, USA (36° 9′ 28″ N, 114° 36′ 28″ W) and the Mojave National Preserve (MNP), California, USA (35° 18′ 3″ N, 115° 33′ 10″ W; Fig. 1a). We selected 22 upland plots in the LMNRA and 4 upland plots in the MNP, each 50 × 50 m (See Supplementary file for plot locations and characteristics). Elevation of the LMNRA plots ranged from 373 to 1000 m above sea level (ASL) and annual precipitation ranged from 11.4 to 19 cm. The MNP plots were at an elevation of 1500 m ASL and averaged 26 cm of precipitation yearly (WorldClim, 2005). Plot slopes ranged from 0 to 13°.

Vegetation in the selected plots was semi-arid shrublands typical of the Mojave Desert Major Land Resource Area (Natural Resource Conservation Service, 2006). The plots were selected to capture a range of variability of plant community composition and ground cover (see Duniway et al., 2011). Dominant shrubs in the LMNRA plots included creosote bush (*Larrea tridentata* (DC.) Coville), catclaw acacia (*Acacia greggii* A. Gray) and burrobush (*Ambrosia dumosa* (A. Gray) Payne). The MNP plots were dominated by blackbrush (*Coleogyne ramosissima* Torr.) and Joshua tree (*Yucca brevifolia* Engelm.).

2.2. Field vegetation measurements

Field measurements of vegetation were taken at the plot level and the individual shrub scale. Plot-level measurements were made in March 2009 as part of a project comparing field and image-derived estimates of vegetation cover (Duniway et al., 2011). These data were used here to evaluate how well stereo imagery could be used to estimate average vegetation height and height diversity within a field plot. In December 2011 (2 years and 9 months after image acquisition, see below), we measured height and crown characteristics of individual shrubs in five LMNRA plots to assess the ability to estimate maximum shrub height, mean height, and crown area from stereo imagery.

Vegetation cover proportions and heights were measured in March 2009 using the line point intercept with heights method described by Herrick et al. (2009). At each plot, six evenly-spaced 50-m transect lines were oriented in a north and south direction. Vegetation intercepting a 1-mm diameter pin was recorded to the species every meter along each transect (300 samples/plot). All vegetation and ground cover that intercepted the pin was recorded, though only the first interception (i.e., top hit) was used for this

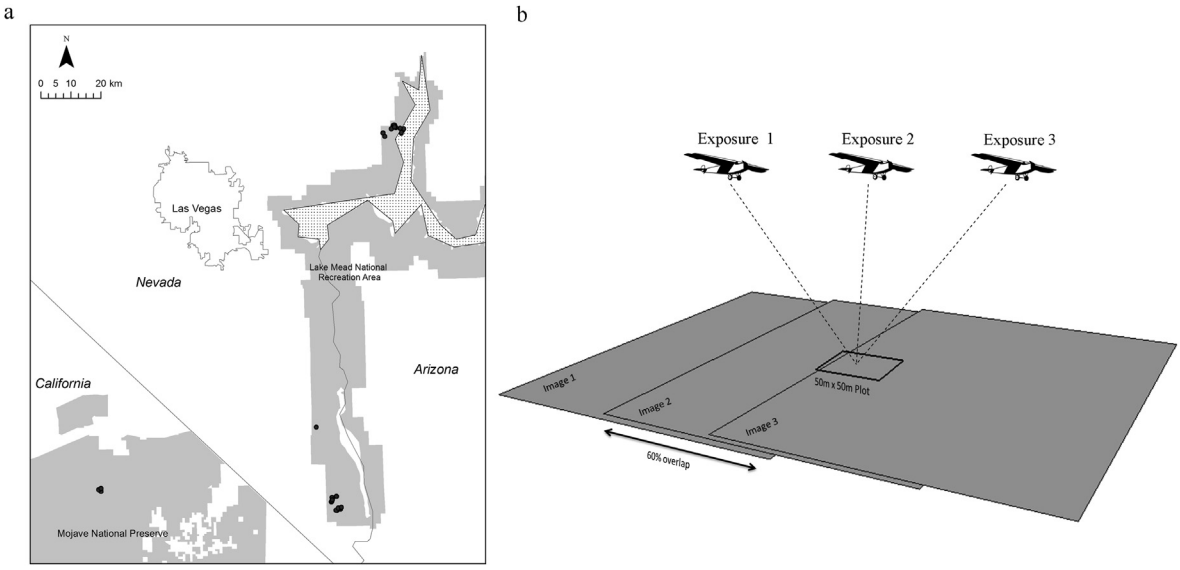

Fig. 1. a) The study area was comprised of 50 m × 50 m vegetation plots, 22 of which were located in the Lake Mead National Recreation Area, Nevada, USA, and 4 were located in the Mojave National Preserve, California, USA. Black dots represent each of the 26 plots. b) Three overlapping color-infrared aerial images with ~60% overlap were acquired for each plot in March 2009.

study. Vegetation was grouped into two categories: woody (shrubs, sub-shrubs, succulents, trees) and non-woody (grasses, forbs).

Vegetation heights (woody and herbaceous) were recorded every 5 m along each transect (60 sample/plot) using a 170 cm long aluminum rod and a circular plexiglass disk of 15-cm radius, weighing 385 g. Two height measurement methods were employed. First, following Herrick et al. (2009), the disk was slowly lowered down the rod until it touched the tallest vegetation and the height at the bottom of the disk recorded to the nearest cm (maximum height method). Second, following Karl and Nicholson (1987, see also Gonzalez et al., 1990), the disk was then raised ~5 cm above the tallest vegetation within 15 cm of the rod and allowed to freefall. The point at which the disk stopped was then measured to the nearest cm (drop-disk method). All vegetation, live or dead, was included in these measurements.

We conducted the individual shrub height measurements at five LMNRA plots in December 2011. We measured 27 shrubs (13 catclaw acacia, 12 creosote bush, and 2 burrobush). These species were chosen because they were the most common within the plots and exhibited very different growth forms (e.g., tall and sparse to short and dense). We stratified our sampling of shrubs into small (12), medium (9), and large (6) to test our ability to accurately estimate heights for varying shrub sizes. For each shrub we measured its maximum height, longest canopy diameter, and the canopy diameter perpendicular to the longest axis to estimate crown area using an elliptical model (see Rittenhouse and Sneva, 1977). To estimate mean height of each shrub, we used a minimum of 25 systematically spaced height measurements using a marked rod and a 10 × 10 cm plastic disk. The disk was lowered down the rod until the tallest vegetation touched it. This height was recorded to

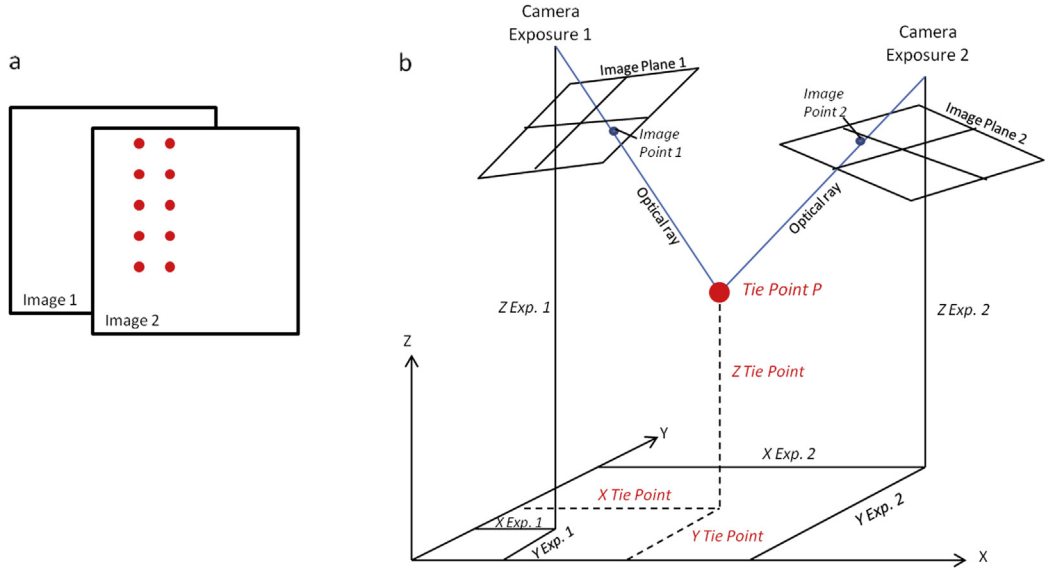

Fig. 2. a) Tie points (red dots) are ground objects that can be identified in multiple overlapping images b) Principles of aerial triangulation: using known internal camera dimensions, coordinates of the camera and the airplane orientation (roll, pitch, yaw) at the time of exposure, we can calculate the X, Y, and Z ground coordinates of the tie points (in red). Figure adapted from Erdas 2009. (For interpretation of the references to color in this figure legend, the reader is referred to the web version of this article.)

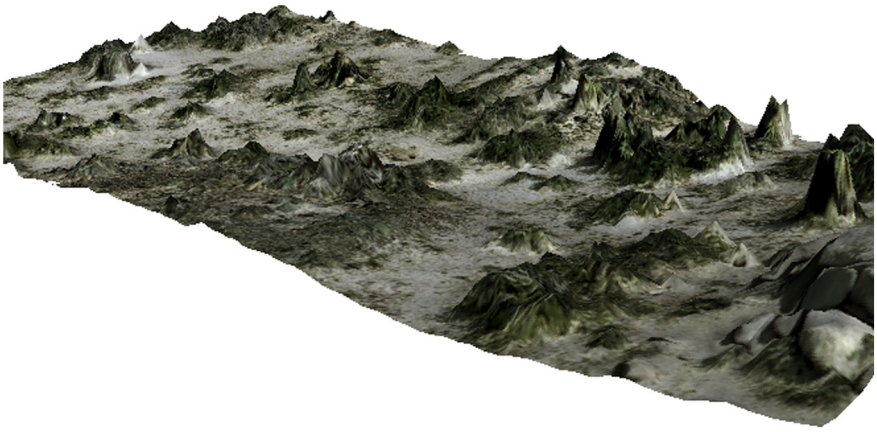

Fig. 3. Imagery draped over reconstructed 3D digital surface model created through aerial triangulation of overlapping images. 1 cm on the image ~ 1 m on the ground.

the nearest cm. Heights were read every 20 cm for small shrubs and every 40 cm for larger shrubs. Because the field measurements were conducted 2 years and 9 months after image acquisition, there could be a marginal mismatch with the imagery due to shrub growth or other environmental factors.

2.3. Image acquisition

Three overlapping color-infrared aerial images were acquired for each plot in March 2009 from a fixed wing Cessna aircraft. The images were taken using the digital frame camera UltraCamX (Vexcel Imaging; Graz, Austria) at a flying height between 333 and 474 m above ground level (AGL), yielding a ground sample distance (GSD) of 2 cm–3 cm. All images we acquired within 2 h of solar noon to minimize shadows. Images included four spectral bands (blue [445–515 nm], green [510–590 nm], red [600–680 nm], near infrared [710–830 nm]) and were recorded at 16-bit depth. The three overlapping images were acquired on a single pass taken approximately 2 s apart to produce ~60% overlap (Fig. 1b). Each image had a ground footprint of approximately 215 m (along track) x 330 m (cross track). Precise camera coordinates and aerial orientation was measured using an Applanix

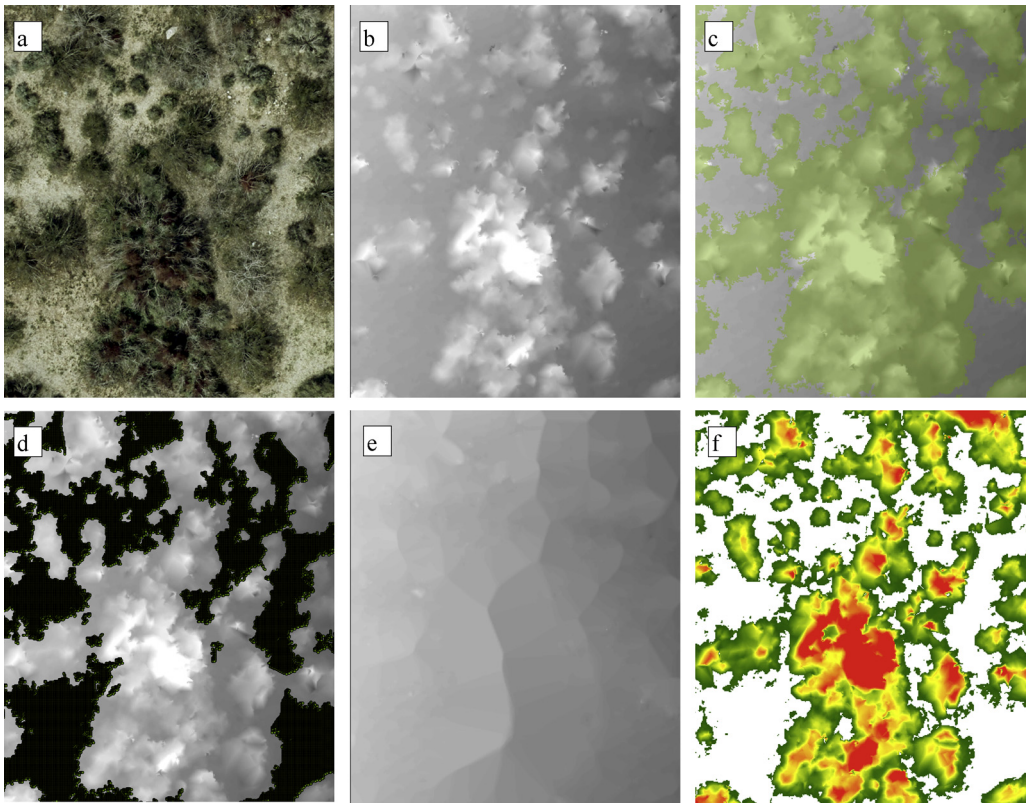

Fig. 4. The image workflow to measure vegetation heights from high-resolution (HR) stereo aerial imagery: a) a single raw HR true color image with 2.3 cm ground-sampling distance (GSD); b) a digital surface model (DSM, 5 cm GSD) was created from overlapping HR stereo aerial imagery by aerial triangulation; c) vegetation (green) was identified and hand digitized into a polygon layer; d) all pixels in the DSM were converted to points and those representing vegetation were deleted, leaving only points that represent the ground elevation; e) an interpolation method was employed with the remaining ground points to estimate the unknown ground elevations underneath the vegetation and create a digital terrain model (DTM); f) the DTM was subtracted from the DSM on a pixel by pixel basis to create a vegetation heights layer.

POS AV (Leek Crescent Richmond Hill, ON Canada) global navigation satellite system (GNSS) and inertial measurement unit (IMU). All image acquisition, georeferencing and production of a single orthorectified image for each plot was completed by Aerographics Inc. (Salt Lake City, UT).

2.4. 3D surface model reconstruction

Viewing a single point on the ground from multiple aerial perspectives (i.e. overlapping images) allows us to measure the height of ground features. Aerial triangulation is the basis for quantitatively deriving these heights by establishing a geometric relationship between the image, the camera, and the ground, from multiple perspectives. The required inputs include the camera dimensions (focal length, physical pixel size), the X, Y, and Z coordinates of the camera at the time of exposure, the airplane orientation (roll, pitch, yaw), and usually precise coordinates of ground control points. A set of distinctive points (tie points) that can be identified in the overlapping portion of each of the images are defined (Fig. 2a). The tie points could be a ground feature such as a rock, shrub, or any other object identifiable in all of the images. The X, Y, and Z ground coordinates of these tie points are then estimated based on the angular relationships inherent in the geometric model created from the known inputs (Fig. 2b). Because the camera, the image point (specific pixels), and the tie point occur along a straight line optical ray, the ground coordinates of the tie point are where the optical rays from each exposure station intersect.

The model inputs including those gathered from the GNSS/IMU system will have some small location error associated with them (up to 0.3 m in our system). In aerial triangulation, if reliable and precise ground control points are available, the actual positions and orientations of the camera can be determined. If ground control points are not available, however, we are left using the initial estimates of the inputs which could lead to inaccurate calculations of ground feature heights, especially at the cm scale. Fortunately, it is possible to reduce the total error by creating a triangulation model that is relatively correct as opposed to absolutely correct. In a relative model, the X, Y, and Z output coordinates will not be correct in reference to sea level, but correct within the model itself. For both model types, the triangulation is carried out using a least-squares bundle-block method. This is an iterative approach that distributes the error across the model and seeks to minimize the deviation between input values and the calculated values. In an absolute model, errors can propagate from each of the three exposure stations to calculate the coordinates of the tie points. In a relative model, we state that the first exposure station has no position or orientation error, while the remaining two stations are allowed to change during the iterative process. This essentially eliminates the error potential from one source but with a consequence of producing outputs in a coordinate system that does not correspond to the real world. This will, however, work for our purposes as we can measure vegetation heights from within the relative model.

Table 1
Individual shrub comparisons between imagery and field measurements using least squares linear regression.

Independent variable	Dependent variable	r	RMSE	Intercept	Slope	$P_{(\text{slope} = 0)}$
Imagery maximum height	Field maximum height	0.709	41.791 cm	92.097	0.715	<0.001
Imagery mean height	Field mean height	0.632	22.199 cm	53.258	1.209	<0.001
Imagery crown area	Field crown area	0.940	1.718 m^2	0.990	1.019	<0.001

Once the geometric model has been established through aerial triangulation, a process called digital image matching looks at each pixel in an image and finds the matching pixels in the other overlapping images. Precise matching is aided by model geometry and the correlation of gray-scale pixels within a neighborhood of the pixel of interest. The X, Y, and Z coordinates of each of these pixels are calculated in the same way as the tie points (Fig. 2b). The final step is to create a spatial data layer that represents these coordinates.

From the overlapping images, we performed aerial triangulation and digital image matching to create 3D digital surface models

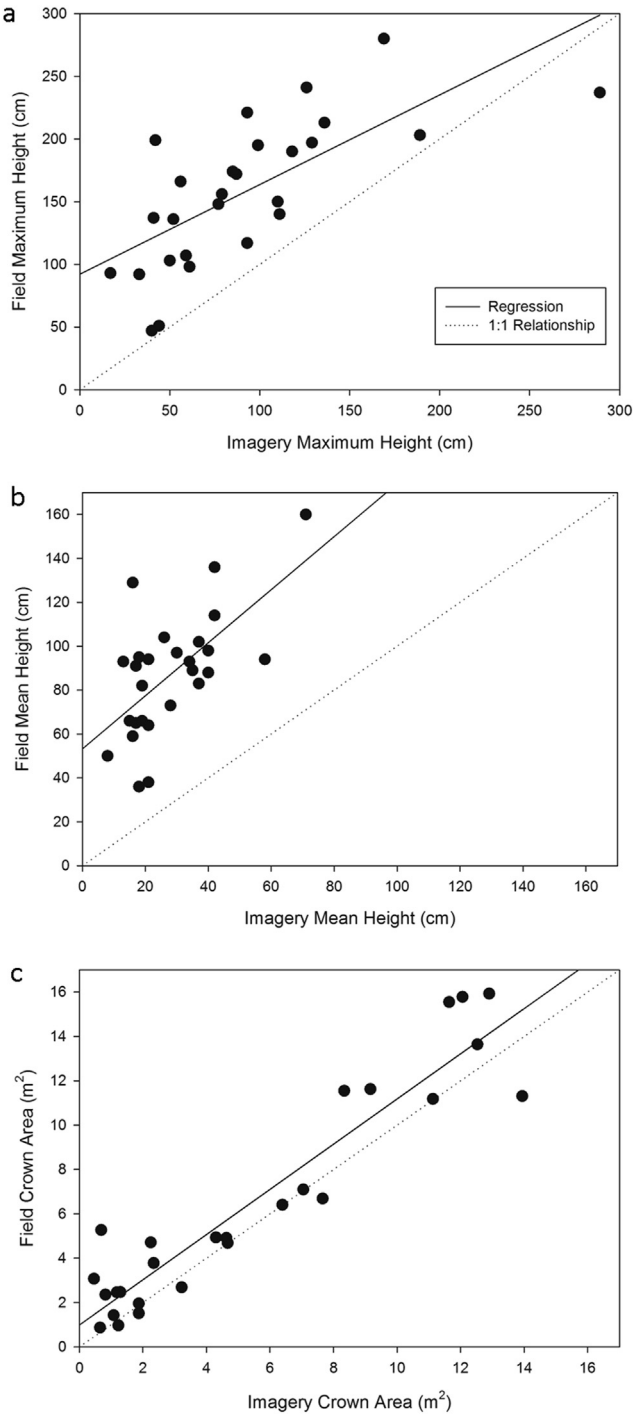

Fig. 5. Comparing imagery and field measurements of individual shrubs using least squares linear regression for a) maximum height b) mean height and c) crown area.

Table 2
Individual shrub image-to-field ratio Kruskal–Wallis one-way analysis of variance on ranks.

Category	*N*	Median	DF	*H* Value	*P* Value
Max height					
Shrub Size	27		2	4.028	0.133
Small	12	0.487			
Medium	9	0.638			
Large	6	0.612			
Species	27		2	3.819	0.148
Burrobush	2	0.857			
Creosote bush	12	0.507			
Catclaw acacia	13	0.523			
Mean height					
Shrub Size	27		2	4.802	0.091
Small	12	0.266			
Medium	9	0.309			
Large	6	0.406			
Species	27		2	4.962	0.084
Burrobush	2	0.526			
Creosote bush	12	0.298			
Catclaw acacia	13	0.328			
Crown area					
Shrub Size	27		2	0.667	0.717
Small	12	0.751			
Medium	9	0.944			
Large	6	0.864			
Species	27		2	5.402	0.067
Burrobush	2	1.248			
Creosote bush	12	0.776			
Catclaw acacia	13	0.810			

(DSM, 5 cm GSD) of each plot using LPS 2010 (ERDAS Norcross, GA; Fig. 3). Approximately 600 tie points were identified in each image set using an automated LPS algorithm. We did not collect ground control points as this would defeat the purpose of using remote sensing to reduce field visits and total project costs. Accordingly, we generated a relative 3D DSM. We fixed the coordinates of the first exposure station as if they had no error and also fixed just the X coordinate of the second image to establish a fixed scale for the model which related image distance to ground distance. The output was a raster spatial data layer.

In ideal cases, when the aerial triangulation inputs are error-free, planimetric (σ_X, σ_Y) and height (σ_Z) accuracies of ground coordinates are estimated using the following equations:

$$\sigma_X = \sigma_Y = \sigma_p * S \quad (1)$$

$$\sigma_Z = \sigma_p * S * \frac{H}{B} \quad (2)$$

Where: H is the flying height, B is the distance between the centers of two successive images, S is the image scale, and σ_p is the parallax accuracy estimated as $\sqrt{2}\sigma_i$, where σ_i is the standard error of the image coordinate measurements in two photos, generated while choosing tie points. The standard error of the image coordinates measurements is usually a function of the image resolution and the level at which we can detect point features in the images. For most automatic tie point detection algorithms σ_i averages $^1/_3$ of the camera physical pixel size. For this study the flight height (H) was 400 m AGL, the distance between the centers of two successive images (B) was approximately 86 m, the image scale (S) was 1:3194, and σ_i was 0.33 pixels. For the UltraCamX, the physical pixel size is 7.2 μm. Substituting these numbers in equations (1) and (2), the expected accuracies for the ground points are $\sigma_X = \sigma_Y = 1.1$ cm and $\sigma_Z = 4.9$ cm, respectively. Actual accuracy for each image set varied depending on the accuracy of the inputs, but the average was $\sigma_X = \sigma_Y = 1.2$ cm (range 0.5–1.8 cm) and $\sigma_Z = 4.5$ cm (range 2.8–6.4 cm).

2.5. Calculating vegetation heights

The DSMs we created represent the heights of all objects on the surface including vegetation, rocks, and the ground. To measure just vegetation, we first needed to identify and remove all of the vegetation features and then interpolate the ground surface height under the vegetation (Fig. 4). We digitized vegetation from the original aerial images draped over each DSM using ArcGIS 10.0 (ESRI Redlands, CA). All vegetation that was at least 5 cm higher than the surrounding area was hand digitized into a polygon layer. The DSM was then converted into a point cloud with one point representing each of the 5 cm pixels. Points within the vegetation polygons were deleted. We then used inverse distance weighting interpolation to estimate ground heights beneath vegetation canopies (Watson and Phillip, 1985). This created an approximate digital terrain model (DTM, or bare-earth model). The DTM was subtracted from the DSM to create a layer of vegetation heights.

2.6. Comparing field and image vegetation heights

Using the vegetation heights layer, we identified each of the individual shrubs that were measured in the field. We recorded from the vegetation heights layer each shrub's maximum height and estimated crown area from measurements of the diameter along the longest axis and the perpendicular axis. Crown area measurements were used to assess the ability of our methods to capture the footprint of the shrub. To estimate the average height of each shrub, we first ran a block-statistic routine (i.e., non-

Table 3
Plot-level vegetation height comparisons between imagery and field measurements using least squares linear regression.

Independent variable	Dependent variable	*r*	RMSE	Intercept	Slope	$P_{(slope = 0)}$
Imagery mean height	Field mean height (maximum height method)	0.746	13.994 cm	17.964	1.473	<0.001
Imagery mean height	Field mean height (drop-disk method)	0.883	4.232 cm	6.727	0.746	<0.001
Woody cover proportion	Image-to-field ratio (maximum height method)	0.701	0.143	0.0472	1.038	<0.001
Woody cover proportion	Image-to-field ratio (drop-disk height method)	0.665	0.304	0.177	2.005	<0.001
Vegetation cover proportion	Image-to-field ratio (maximum height method)	0.370	0.186	0.138	0.294	0.063
Vegetation cover proportion	Image-to-field ratio (drop-disk height method)	0.472	0.359	0.272	0.764	0.015
Imagery standard deviation	Field standard deviation (maximum height method)	0.723	12.980 cm	19.530	0.995	<0.001
Imagery standard deviation	Field standard deviation (drop-disk height method)	0.620	7.625 cm	14.245	0.442	<0.001

overlapping moving-window analysis) on the imagery to find the highest value within a 10 cm × 10 cm window around each pixel. This was done to more closely match the sampling method in the field which recorded the highest vegetation that intercepted a 10 cm × 10 cm disk. These heights were averaged for each shrub individually.

At the plot level we replicated the sampling design of the field work by generating 60 systematically-placed points each buffered by a circle with a radius of 15 cm. The greatest vegetation height within the circle was recorded, and these heights were averaged over all 60 points per plot. The 60 systematic points were not intended to sample the same locations that were measured in the field, but to mirror the field method as closely as possible. Comparisons of field and image data were done at the plot-level, not on a point-by-point basis.

2.7. Analysis

We used Pearson correlations to determine the strength of the relationship between the image and the field measurements. To assess the accuracy of our vegetation height modeling we compared image and field measurements using least squares linear regression. For individual shrubs, we ran regressions for maximum height, mean height, and crown area. To assess if accuracy differed between shrub size and species, we conducted analyses of variance (ANOVAs) comparing a ratio of image-measured to field-measured values (*image measurement/field measurement*) for shrub size and species separately. We used the Kruskal–Wallis non-parametric one-way ANOVA on ranks because some of the data exhibited uneven variances.

At the plot level we ran Pearson correlations and linear regressions comparing field measurements to image-estimates for mean and standard deviation vegetation heights. To determine if the amount and composition of vegetation cover affected our ability to estimate vegetation heights, we compared the ratio of plot-level image to plot-level field measured height with the total vegetation cover and also cover of woody vegetation using linear regression. Finally, we compared the image-to-field measurement ratio by dominant shrub species for each plot to see if image-based estimates were more successful in certain shrub communities. A ratio of 1 indicated very good accuracy. All of the plot-level analyses were conducted using the maximum height field method and the drop-disk field method.

3. Results

3.1. Individual shrubs

For individual shrub maximum height we found a moderately strong linear relationship between heights measured in the field and those estimated from the imagery (r = 0.709, RMSE = 41.791 cm; Table 1, Fig. 5a). Imagery measurements, however, were always lower than field estimates, except for one shrub. Image-to-field height ratios for maximum height averaged 0.58 but ranged from 0.18 to 1.21. Larger shrubs on average had better image-to-field ratios compared with smaller shrubs, yet these differences were not statistically significant with $\alpha = 0.05$ (Table 2). Image-to-field height ratios by species also did not show any significant differences. However, burrobush, a compact and dense shrub, had ratios closest to 1 than any species, (0.85 and 0.86) though only two shrubs of this species were sampled.

Mean height for individual shrubs was significantly underestimated by the imagery measurement technique (Fig. 5b), and showed a poorer relationship to field measurements than other shrub metrics (r = 0.632, RMSE = 22.199 cm; Table 1). Image-to-field height ratios for mean height averaged 0.32 (range 0.12–0.61). Larger shrubs on average had better image-to-field ratios compared with smaller shrubs, yet these differences were

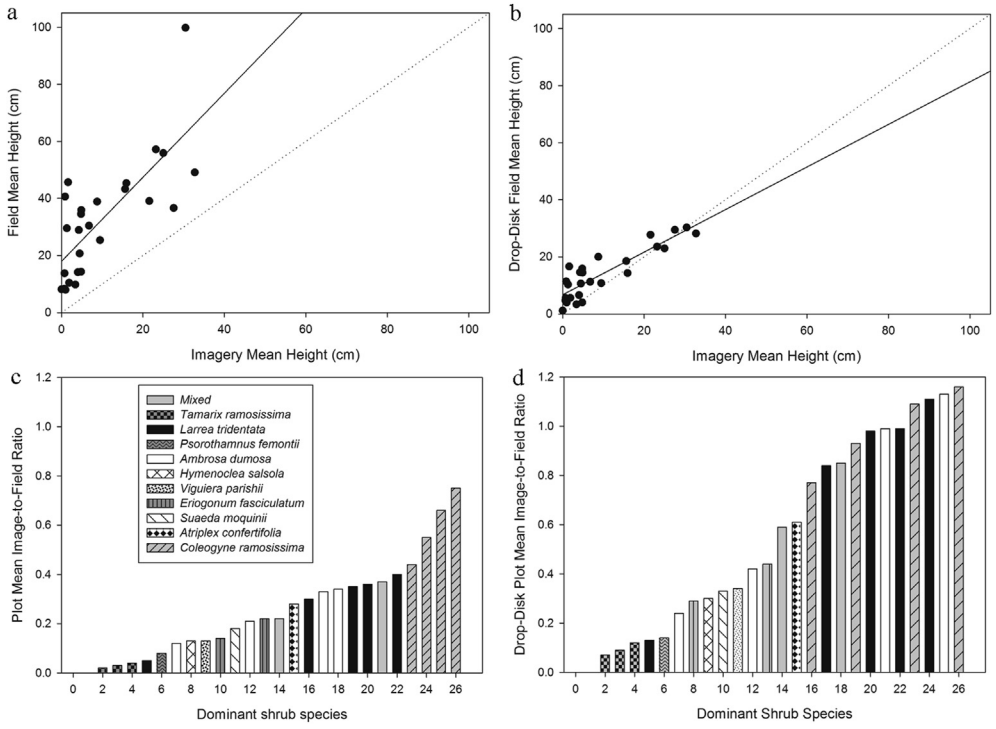

Fig. 6. a) Comparing plot mean between imagery and maximum height field method using least squares linear regression b) Comparing plot mean between imagery and drop-disk field method using least squares linear regression c) Plot mean image-to-field ratio between the maximum height field method and the imagery symbolized by dominant shrub species d) Plot mean image-to-field ratio between the drop-disk field method and the imagery symbolized by dominant shrub species.

not statistically significant (Table 2). Compact shrubs like burrobush had relatively high ratio values (0.5 and 0.55) whereas creosote bush and catclaw acacia had lower averages. Differences between shrub species were not statistically significant.

Image-based estimates of crown area for individual shrubs more closely matched field measurements than did the height metrics, but were still on average lower than field-based estimates. There was a strong linear relationship between the field and image based methods ($r = 0.940$, RMSE 1.718 m^2; Table 1, Fig. 5c). Image-to-field ratios for crown area averaged 0.81 (range 0.13–1.26). Burrobush had high image-to-field ratios (1.22 and 1.26) that actual overestimated the crown area. Larger shrubs were again modeled better than smaller shrubs. However, neither species nor size had any significant differences (Table 2).

3.2. Plots

At the plot level, image estimates of vegetation height were also lower than field height measurements. Using the maximum height method, there was a moderately strong linear relationship between image-estimated and field measured mean height ($r = 0.746$, RMSE 13.994 cm), but that relationship was much stronger with the drop-disk method ($r = 0.883$, RMSE 4.232 cm), which removed much of the influence of sparse vegetation or thin branches at the top of the canopy (Table 3, Fig. 6a, b). Plot level image-to-field ratios using the maximum height field method averaged 0.25 (range 0–0.75; Fig. 6c) while ratios with the drop-disk field method were much better with an average of 0.57 (range 0–1.16; Fig. 6d). The dominant shrub species within the plots affected the image-to-field ratios for both field methods. Plots dominated by saltcedar (*Tamarix ramosissima* Ledeb.), a shrub with a very thin crown structure, were modeled very poorly compared with the field methods. Conversely, plots dominated by shrubs such as blackbrush, creosote bush, and burrobush, which typically grow in a more compact form, were modeled better.

We found a positive linear relationship between plot level image-to-field ratios and woody cover proportion (Table 3) using the maximum height method ($r = 0.701$, RMSE 0.143) and the drop-disk method ($r = 0.665$, RMSE 0.304). Total vegetation cover (Table 3), however, was a weak indicator of plot level image-to-field ratios using the maximum height method ($r = 0.370$, RMSE 0.186), and the drop-disk method ($r = 0.472$, RMSE 0.359).

Standard deviation of vegetation heights within plots (a measure of height diversity) was on average lower in the imagery (16.36 cm) than in the maximum height field method (35.81 cm) and the drop-disk field method (21.47 cm). There was a moderately strong linear relationship between imagery and the maximum height field method standard deviations ($r = 0.723$, RMSE 12.98 cm; Table 3, Fig. 7a), which is very comparable to the relationship for mean height of the plot. However, using the drop-disk field method, the image-to-field relationship of standard deviation was weaker than the maximum height method ($r = 0.620$, RMSE 7.62 cm; Table 3, Fig. 7b). This result was affected by poor correlation in the plots dominated by saltcedar.

Histograms of all the height measurements across all plots for each method, illustrated how the diversity of heights differed between the imagery and field methods while minimizing the influence of any one plot (Fig. 7c). The histogram for image-based heights was fairly similar to the drop-disk histogram except in the ≤5 cm bin where there were 123 more samples. Most of the herbaceous vegetation (grasses and forbs) could not be identified in the imagery, and were therefore assigned to the ≤5 cm bin. The same phenomenon was even more pronounced comparing the imagery heights to the maximum height field method with a difference of 578 samples in the ≤5 cm bin.

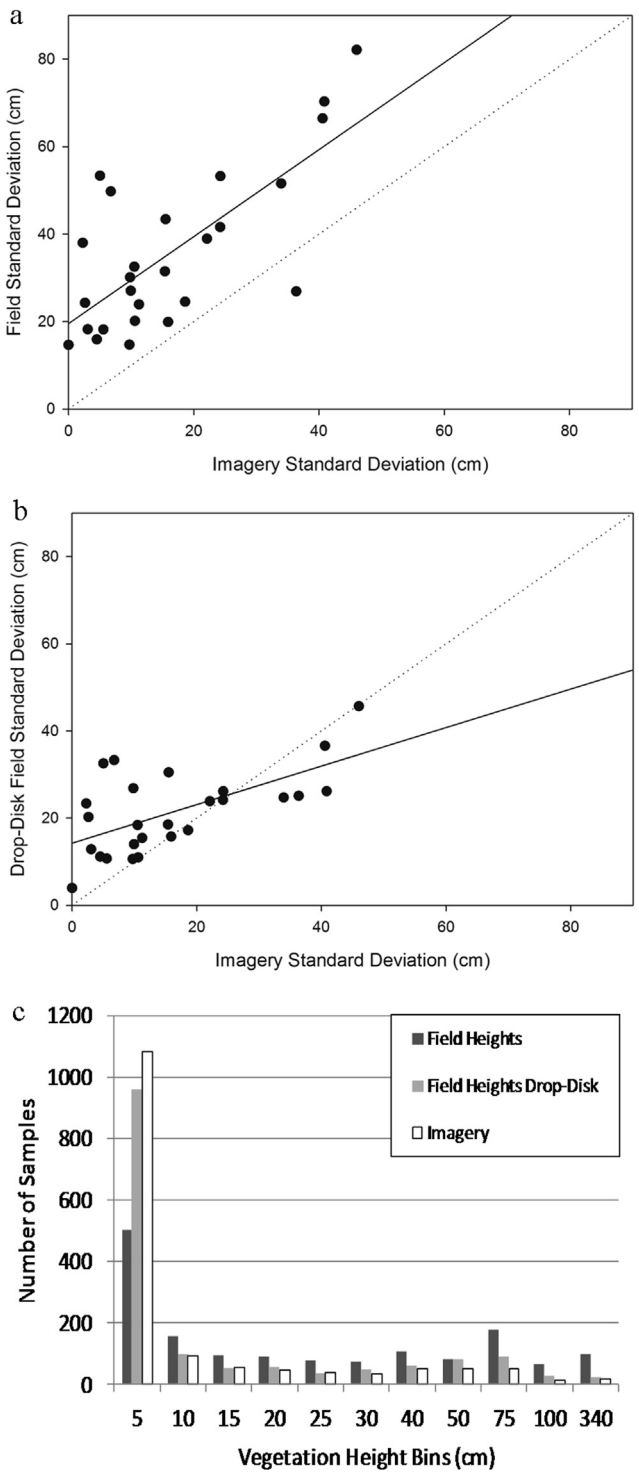

Fig. 7. a) Comparing plot standard deviation between the imagery and the maximum height field method using least squares linear regression b) Comparing plot standard deviation between the imagery and the drop-disk field method using least squares linear regression c) Histogram of all height measurements in all plots combined ($n = 1513$) from the imagery, the maximum field heights method, and the drop-disk field method.

4. Discussion

Our results demonstrate the potential to use high-resolution digital stereo imagery to estimate heights of shrubs and characterize plot-level vegetation structure within some limitations.

While modeling large shrubs was generally more successful than small shrubs, the density (i.e., compactness) of a shrub appeared to be the most important factor estimating its height from imagery. This is well illustrated by two examples (Fig. 8). Shrubs with a dense crown or compact shape are more likely to match the field measurements while shrubs with sparse growth forms and thin branches are likely to be greatly underestimated, regardless of size. We found good height estimates for compact, dense shrubs like burrobush and plots dominated by blackbrush. This suggests that stereo-image height estimation might do well in other systems featuring dense shrubs like sagebrush (*Artemisia* spp.) or juniper (*Juniperus* spp.).

Successful characterization of plot-level vertical structure depended not only on the types of shrubs present but also overall species composition in the plot. Grasses and forbs were generally too small to be adequately modeled with the resolution of imagery we used. Therefore, estimates of vertical structure will be more accurate in plots having low herbaceous cover and high amounts of dense shrubs.

In almost all cases image-based estimates of height were lower than field-based measurements. This result is not unique to our study. Glenn et al. (2011), Mitchell et al. (2011), and Streutker and Glenn (2006) all reported underestimation of shrub heights from LiDAR data in sagebrush steppe environments. All of these studies used a maximum height method for recording vegetation height in the field. Differences in how vegetation was observed and measured in the field versus how it appears in the imagery may contribute to underestimation of heights using remote sensing or photogrammetric techniques. With the exception of the drop-disk method, field measurement methods record the height of the tallest vegetation encountered. This often was a thin branch or leaf that extended above the main shrub canopy. Even with high-resolution imagery, many of these small branches get filtered out, leaving only the main canopy. The result is a mismatch in how vegetation height is perceived between the two methods. This definition discrepancy was compounded when estimating mean shrub height through multiple measurements. With more research and calibration it may be possible to develop standard corrections for relating field-measured and stereo-image-estimated heights for different shrub canopy structures. However, the adoption of a field technique that better matches the stereo-image characteristics may be a better option.

The drop-disk method of measuring vegetation height is more in line with how vegetation is represented by the DSM and gave much better relationship to stereo-image heights at the plot level. Drop-disk methods have been shown reliable for estimating plant attributes like crown area or aboveground biomass for agricultural as well as natural systems (Bransby et al., 1977; Karl and Nicholson, 1987; Gonzalez et al., 1990) but have not seen widespread use outside of agricultural applications. Use of maximum height methods in monitoring programs like the NRI or BLM's AIM may be due to their inherent simplicity (i.e., not needing special equipment just for measuring height) and objectivity (i.e., observers easily trained and results consistent between observers). Drop-disk methods require more effort to implement due to equipment requirements, additional training for observers, and the need to calibrate to site conditions (Karl and Nicholson, 1987). However, if a technique like drop-disk height more closely matches how vegetation height is estimated from remotely-sensed products, then it may be worth the effort.

5. Conclusion

High resolution digital photogrammetry is a promising yet under-researched tool for measuring vegetation structure in arid and semi-arid ecosystems. Though improvements are needed in DTM automation and relating field-to-image measurements, this technology could be useful for broad-scale monitoring and

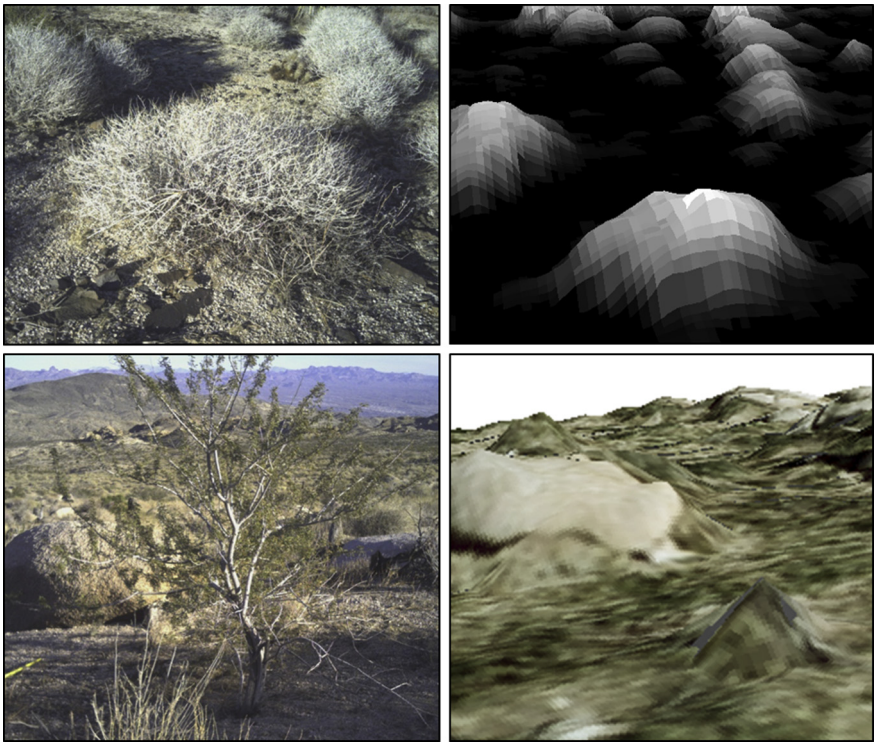

Fig. 8. The top two images show that dense or compact shrubs (*Ambrosia dumosa* pictured here) can be modeled with minor underestimation, regardless of size. The bottom two images show that thin shrubs with long branches (*Acacia greggii* pictured here) are more difficult to model accurately.

assessment. With the popularity of sensors like LiDAR in the published literature, photogrammetry may be seen as an "old-fashioned" way of getting height information. However, many resource monitoring programs are already collecting aerial photography, and with some modifications (e.g., digital image acquisition, higher resolution imagery, adequate image overlap) vegetation heights could be extracted from that imagery. Also, photogrammetric methods could be used on historical or archived stereo imagery for retrospective vegetation studies. Unmanned aerial systems (UAS) for collecting aerial imagery, a technology that is seeing increasing application in natural resource monitoring (Laliberte et al., 2010, 2011), could provide a less expensive and safe means for collecting high-resolution stereo imagery.

Acknowledgments

This project was funded, in part, through the USDA-NRCS Conservation Effects Assessment Project (CEAP). We are grateful for assistance provided by staff at the National Park Service Lake Mead National Recreation Area and Mojave Desert Network. M. Mattocks and N. Baquera assisted in collection of the field data. Any use of trade, product, or firm names is for descriptive purposes only and does not imply endorsement by the U.S. Government.

Appendix A. Supplementary data

Supplementary data related to this article can be found at http://dx.doi.org/10.1016/j.jenvman.2014.05.028.

References

Asner, G.P., Archer, S., Hughes, R.F., Ansley, R.J., Wessman, C.A., 2003. Net changes in regional woody vegetation cover and carbon storage in Texas drylands, 1937–1999. Glob. Change Biol. 9 (3), 316–335.
Booth, T.D., Cox, S.E., 2008. Image-based monitoring to measure ecological change in rangeland. Front. Ecol. Environ. 6 (4), 185–190.
Booth, T.D., Glenn, D., Keating, B., Nance, J., Cox, S.E., Barriere, J.P., 2003. Monitoring rangeland watersheds with very-large scale aerial imagery. In: First Interagency Conference on Research in the Watersheds, October 27–30, 2003. U.S. Department of Agriculture, Agricultural Research Service.
Bransby, D.I., Matches, A.G., Krause, G.F., 1977. Disk meter for rapid estimation of herbage yield in grazing trials. Agronomy J. 69 (3), 393–396.
Brown, S., Pearson, T., Slaymaker, D., Ambagis, S., Moore, N., Novelo, D., Sabido, W., 2005. Creating a virtual tropical forest from three-dimensional aerial imagery to estimate carbon stocks. Ecol. Appl. 15 (3), 1083–1095.
Bryant, F.C., Kothmann, M.M., 1979. Variability in predicting edible browse from crown volume. J. Range Manag. 32 (2), 144–146.
Cleary, M.B., Pendall, E., Ewers, B.E., 2008. Testing sagebrush allometric relationships across three fire chrono sequences in Wyoming, USA. J. Arid Environ. 72 (4), 285–301.
Connelly, J.W., Schroeder, M.A., Sands, A.R., Braun, C.E., 2000. Guidelines to manage sage grouse populations and their habitats. Wildl. Soc. Bull. 28 (4), 967–985.
Duniway, M.C., Karl, J.W., Schrader, S., Baquera, N., Herrick, J.E., 2011. Rangeland and pasture monitoring: an approach to interpretation of high-resolution imagery focused on observer calibration for repeatability. Environ. Monit. Assess. 184 (6), 3789–3804.
Erdas, Inc, 2009. LPS project manager User's Guide. Norcross, Ga, USA.
Glenn, N.F., Spaete, L.P., Sankey, T.T., DerryBerry, D.R., Hardegree, S.P., Mitchell, J.J., 2011. Errors in LiDAR-derived shrub height and crown area on sloped terrain. J. Arid Environ. 75 (4), 377–382.
Gong, P., Biging, G.S., Standiford, R., 2000. Technical note: use of digital surface model for hardwood rangeland monitoring. J. Range Manag. 53 (6), 622–626.
Gonzalez, M.A., Hussey, M.A., Conrad, B.E., 1990. Plant height, disk, and capacitance meters used to estimate bermudagrass herbage mass. Agronomy J. 82 (5), 861–864.
Green, G.A., Anthony, R.G., 1989. Nesting success and habitat relationships of burrowing owls in the Columbia Basin, Oregon. Condor 91 (2), 347–354.
Herrick, J.E., Lessard, V., Spaeth, K.E., Shaver, P., Dayton, R.S., Pyke, D.A., Jolley, L., Goebel, J.J., 2010. National ecosystem assessments supported by scientific and local knowledge. Front. Ecol. Environ. 8 (8), 403–408.
Homer, C.G., Aldridge, C.L., Meyer, D.K., Schell, S.J., 2012. Multi-scale remote sensing sagebrush characterization with regression trees over Wyoming, USA: laying a foundation for monitoring. Int. J. Appl. Earth Observation Geoinformation 14 (1), 233–244.
House, C.C., Goebel, J.J., Schreuder, H.T., Geissler, P.H., Williams, W.R., Olsen, A.R., 1998. Prototyping a vision for inter-agency terrestrial inventory and monitoring: a statistical perspective. Environ. Monit. Assess. 51 (1), 451–463.
Hunt Jr., E.R., Everitt, J.H., Ritchie, J.C., Moran, M.S., Booth, T.D., Anderson, G.L., Clark, P.E., Seyfried, M.S., 2003. Applications and research using remote sensing for rangeland management. Photogrammetric Eng. Remote Sens. 69 (6), 675–693.
Jakubauskas, M., Kindscher, K., Debinski, D., 2001. Spectral and biophysical relationships of montane sagebrush communities in multi-temporal SPOT XS data. Int. J. Remote Sens. 22 (9), 1767–1778.
Karl, J.W., Duniway, M.C., Schrader, T.S., 2012a. A technique for estimating rangeland canopy-gap size distributions from very-high-resolution digital imagery. Rangel. Ecol. Manag. 65 (2), 196–207.
Karl, J.W., Duniway, M.C., Nusser, S.M., Opsomer, J.D., Unnasch, R.S., 2012b. Using very-large-scale aerial imagery for rangeland monitoring and assessment: some statistical considerations. Rangel. Ecol. Manag. 65 (4), 330–339.
Karl, M.G., Nicholson, R.A., 1987. Evaluation of the forage-disk method in mixed-grass rangelands of Kansas. J. Range Manag. 40 (5), 467–471.
Laliberte, A.S., Browning, D.M., Herrick, J.E., Gronemeyer, P., 2010. Hierarchical object-based classification of ultra-high-resolution digital mapping camera (DMC) imagery for rangeland mapping and assessment. J. Spatial Sci. 55 (1), 101–115.
Laliberte, A.S., Winters, C., Rango, A., 2011. UAS remote sensing missions for rangeland applications. Geocarto Int. 26 (2), 141–156.
Leis, S.A., Morrison, L.W., 2011. Field test of digital photography biomass estimation technique in tallgrass prairie. Rangel. Ecol. Manag. 64 (1), 99–103.
Lucas, R.M., Ellison, J.C., Mitchell, A., Donnelly, B., Finlayson, M., Milne, A.K., 2002. Use of stereo aerial photography for quantifying changes in the extent and height of mangroves in tropical Australia. Wetl. Ecol. Manag. 10 (2), 161–175.
Luscier, J.D., Thompson, W.L., Wilson, J.M., Gotham, B.E., Dragut, L.D., 2006. Using digital photographs and object-based image analysis to estimate percent ground cover in vegetation plots. Front. Ecol. Environ. 4 (8), 408–413.
Massada, A.B., Carmel, Y., Tzur, G.E., Grünzweig, J.M., Yakir, D., 2006. Assessment of temporal changes in aboveground forest tree biomass using aerial photographs and allometric equations. Can. J. For. Res. 36 (10), 2585–2594.
Miller, D.R., Quine, C.P., Hadley, W., 2000. An investigation of the potential of digital photogrammetry to provide measurements of forest characteristics and abiotic damage. For. Ecol. Manag. 135 (1), 279–288.
Mitchell, A.L., Lucas, R.M., Donnelly, B.E., Pfitzner, K., Milne, A.K., Finlayson, M., 2007. A new map of mangroves for Kakadu National Park, Northern Australia, based on stereo aerial photography. Aquatic Conservation: Mar. Freshw. Ecosyst. 17 (5), 446–467.
Mitchell, J.J., Glenn, N.F., Sankey, T.T., DerryBerry, D.R., Anderson, M.O., Hruska, R.C., 2011. Small-footprint Lidar estimations of sagebrush canopy characteristics. Photogrammetric Eng. Remote Sens. 77 (5), 521–530.
National Research Council, 1994. Rangeland Health: New Methods to Classify, Inventory, and Monitor Rangelands. National Academy Press, Washington, D.C.
Natural Resource Conservation Service, 2006. Land Resource Regions and Major Land Resource Areas of the United States, the Caribbean, and the Pacific Basin. United States Department of Agriculture, Washington, D.C.
Nusser, S.M., Goebel, J.J., 1997. The national resources inventory: a long-term multi-resource monitoring programme. Environ. Ecol. Statistics 4 (3), 181–204.
Okin, G.S., 2008. A new model of wind erosion in the presence of vegetation. J. Geophys. Res. 113 (F2). F02S10.
Rango, A., Laliberte, A.S., Herrick, J.E., Winters, C., Havstad, K.M., Steele, C., Browning, D., 2009. Unmanned aerial vehicle based remote sensing for rangeland assessment, monitoring and management. J. Appl. Remote Sens. 3 (1), 033542.
Reutebuch, S.E., Andersen, H.E., McGaughey, R.J., 2005. Light detection and ranging (LIDAR): an emerging tool for multiple resource inventory. J. For. 103 (6), 286–292.
Riaño, D.E., Chuvieco, E., Ustin, S.L., Salas, J., Rodríguez-Pérez, J.R., Ribeiro, L.M., Viegas, D.X., Moreno, J.M., Fernández, H., 2007. Estimation of shrub height for fuel-type mapping combining airborne LiDAR and simultaneous color infrared ortho imaging. Int. J. Wildland Fire 16 (3), 341–348.
Rittenhouse, L.R., Sneva, F.A., 1977. A technique for estimating big sagebrush production. J. Range Manag. 30 (1), 68–70.
Sankey, T.T., Bond, P., 2011. LiDAR-based classification of sagebrush community types. Rangel. Ecol. Manag. 64 (1), 92–98.
Seefeldt, S.S., Booth, T.D., 2006. Measuring plant cover in sagebrush steppe rangelands: a comparison of methods. Environ. Manag. 37 (5), 703–711.
Streutker, D., Glenn, N.F., 2006. Lidar measurement of sagebrush steppe vegetation heights. Remote Sens. Environ. 102 (1), 135–145.
Su, J.G., Bork, E.W., 2007. Characterization of diverse plant communities in Aspen Parkland rangeland using LiDAR data. Appl. Veg. Sci. 10 (3), 407–416.
Toevs, G.R., Karl, J.W., Taylor, J.J., Spurrier, C.S., Karl, M.S., Bobo, M.R., Herrick, J.E., 2011. Consistent indicators and methods and a scalable sample design to meet assessment, inventory, and monitoring information needs across scales. Rangelands 33 (4), 14–20.
Watson, D.F., Phillip, G.M., 1985. A refinement of inverse distance weighted interpolation. Geoprocessing 2 (4), 315–327.
Wolf, P.R., Dewitt, B.A., 2000. Elements of Photogrammetry: With Applications in GIS. The McGraw-Hill Companies, Inc.
WorldClim, 2005. Precipitation 30 Arc-second Resolution Version 1.4. http://www.worldclim.org (accessed 20.02.12.).